Supplemental Data

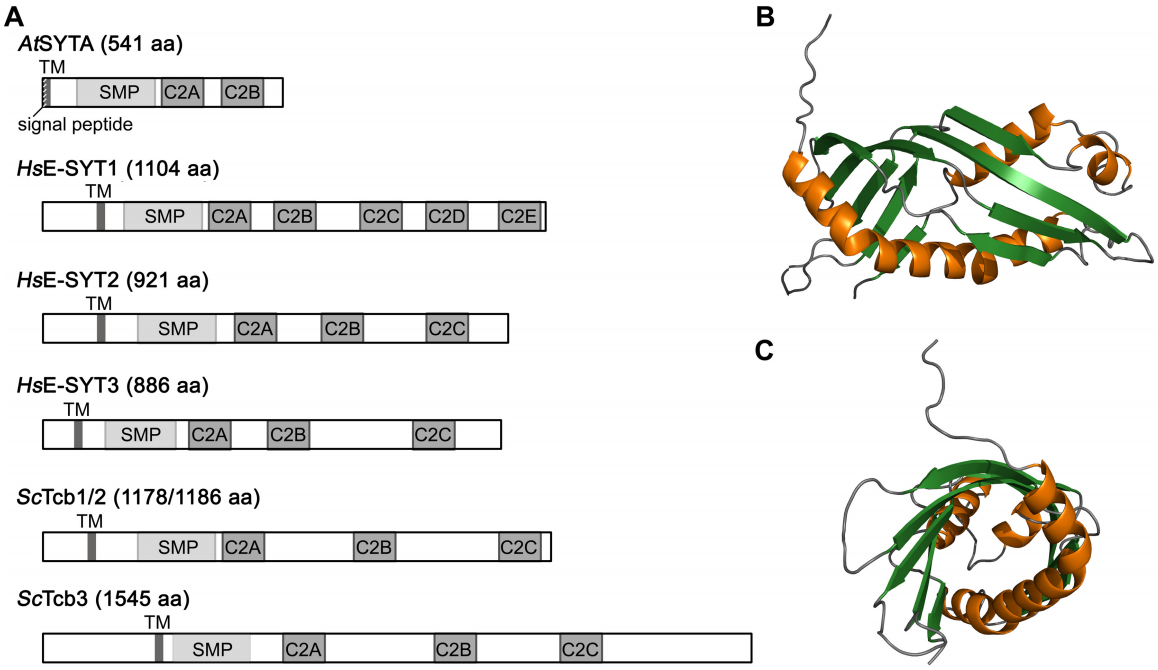

D

```
AtSYTA    VKNPDFDRVDWINRFLEYMWPYLDKAICKTAKNIAKPIIEE--QIPKYKIDSVEFETLTLGSLPPTFQGMKVYL  133
AtSYTB    VKNPDFDRIDWLNKLIGHMWPYMDKAICKMAKSIAKPIIAE--QIPNYKIDSVEFEMLTLGSLPPSFQGMKVYA  135
AtSYTC    MKNPDYERVDWFNKFISYMWPYLDKAVCGIIRSSVQPLFAD--YIGTFCIESIEFENLSLGTLPPTVHGVKFYE  133
AtSYTD    VVFSQRQKLNWLNLELEKIWPYVNEAASELIKSSVEPVLEQ--YTPAM-LASLKFSKFTLGTVAPQFTGVSILE  138
AtSYTE    VVFSERQKLTWLNHHLTKIWPYVDEAASELIKASVEPVLEQ--YRPAI-VASLTFSKLTLGTVAPQFTGVSVID  141
HsE-SYT1  VSFPDVEKAEWLNKIVAQVWPFLGQYMEKLLAETVAPAVRG----SNPHLQTFTFTRVELGEKPLRIIGVKVHP  206
HsE-SYT2  VHFPDTERAEWLNKTVKHMWPFICQFIEKLFRETIEPAVRG----ANTHLSTFSFTKVDVGQQPLRINGVKVYT  256
HsE-SYT3  IHFPDVERVEWANKIISQTWPYLSMIMESKFREKLEPKIRE----KSIHLRTFTFTKLYFGQKCPRVNGVKAHT  184
ScTcb1    KVENDYESLEWLNAFLDKYWPILEPSVSQLIVQQANEQMATNEAIPKF-ITQLWIDELTLGVKPPRVDLVKTFQ  240
ScTcb2    KITSDYESVEWLNTFLDKYWPIIEPSVSQQIVDGTNTALSENVAIPKF-IKAIWLDQFTLGVKPPRIDAIKTFQ  237
ScTcb3    TLSDRVESTTWLNSFLSKFWVIYMPVLSQQVKDNVNPQLAG--VAPGYGIDALAIDEFTLGSKAPTIKGIKSYT  339
                 :  * *  :  *                .       :  . :  . .*    .  :.

AtSYTA    TD--EKELIMEPCLKWAA--------------NPNILVAI---KAF-GLKATVQVVDLQVFAQPRITLKPLVP  186
AtSYTB    TD--DKEIIMELSVKWAG--------------NPNIIVVA---KAF-GLKATVQVIDLQVYATPRITLKPLVP  188
AtSYTC    TN--EKELLFEPSIKWAG--------------NPNIVLVL---KVL-SLRIRVQLVDLQFFAIVRVALKPLLP  186
AtSYTD    SESGPNGITMELEMQWDG--------------NPKIVLDV---KTLLGVSLPIEVKNIGFTGVFRLIFKPLVD  194
AtSYTE    GDK--NGITLELDMQWDG--------------NPNIVLGV---KTLVGVSLPIQVKNIGFTGVFRLIFRPLVE  195
HsE-SYT1  GQ-RKEQILLDLNISYVG--------------DVQIDVEV---KKY---FCKAGVKGMQLHGVLRVILEPLIG  258
HsE-SYT2  ENVDKRQIILDLQISFVG--------------NCEIDLEI---KRY---FCRAGVKSIQIHGTMRVILEPLIG  309
HsE-SYT3  NTCNRRRVTVDLQICYIG--------------DCEISVEL---QK-----IQAGVNGIQLQGTLRVILEPLLV  235
ScTcb1    NT-ASDVVVMDWGISFTPHDLCDMSAKQVRNYVNELAVVKA---KIF-GITIPVSVSDIAFKAHARVKFK-LMT  308
ScTcb2    NT-KSDVVVMDVCLSFTPHDMSDLDAKQCRNYVNSNVVLKA---KIF-GMDIPVSVADIFFQVFVRFRFQ-LMT  305
ScTcb3    KT-GKNTVEMDWSFAFTPSDVSDMTATEAREKINPKISLGVTLGKSFVSKTMPILVEDINVAGKMRIKVE-FGK  411
                : .:  . :                  :    :     :          : .: .    *. .  :

AtSYTA    SFPCFANIYVSLMEKPHVDFGLKLGGADLMS------IPGLYRFVQEQIKDQVANMYLWPKTLVVPIL        248
AtSYTB    SFPCFANIFVSLMDKPQVDFGLKLLGADVMA------IPGLYRFVQEIIKDQVANMYLWPKTLNVQIM        249
AtSYTC    TFPCFGMVVVSLMEKPHVDFGLKVLGGDLMS------IPGLYRYVQETIKRQVSSMYHWPQVLEIPIL        248
AtSYTD    EFPCFGALSYSLREKKGLDFTLKVIGGELTS------IPGISDAIEETIRDAIEDSITWPVRKIIPIL        256
AtSYTE    DFPCFGAVSVSLREKKKLDFTLKVVGGDISA------IPGLSEAIEETIRDAVEDSITWPVRKVIPII        257
HsE-SYT1  DLPFVGAVSMFFIRRPTLDINWTGM-TNLLD------IPGLSSLSDTMIMDSIAAFLVLPNRLLVPLV        319
HsE-SYT2  DMPLVGALSIFFLRKPLLEINWTGL-TNLLD------VPGLNGLSDTIILDIISNYLVLPNRITVPLV        370
HsE-SYT3  DKPFVGAVTVFFLQKPHLQINWTGL-TNLLD------APGINDVSDSLLEDLIATHLVLPNRVTVPVK        296
ScTcb1    PFPHVETVNIQLLKVPDFDFVATLFGRSIFNWEILA-IPGLMTLIQKMAKKYMGPILLPPFSLQLNIP        375
ScTcb2    TLPLVETINIQLLEVPEVDFISRLLGNSVFNWEILA-IPGLMRLIQKMAFKYLSPVLLPPFSLQLNIP        372
ScTcb3    AFPNIKIVSLQLLEPPLIDFALKPIGGDTLGLDVMSFLPGLKSFVKNIINSNIGPMLFPPNHLDINVE        429
            * .  :   :    .::       .          **:    .     :      *    : :
```

E

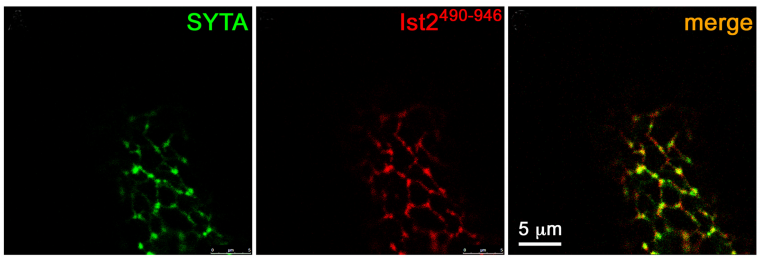

Figure S1. Arabidopsis SYTA contains a predicted SMP domain and co-localizes with the *S. cerevisiae* ER-plasma membrane tethering protein Ist2 when transiently expressed in *N. benthamiana*. Related to Figure 1.

(A) Predicted domain organization of Arabidopsis SYTA, human (*Hs*)E-SYTs 1, 2 and 3, and *Saccharomyces cerevisiae* tricalbins Tcb 1, 2 and 3, with amino acid lengths as indicated. TM, transmembrane domain; SMP, synaptotagmin-like mitochondrial lipid binding protein domain; C2 (lettered), predicted C2-type Ca^{2+}/lipid binding domains. The predicted TM in the three human E-SYTs has been shown to form a hairpin insertion into the ER membrane, with both N- and C-terminal regions being cytosolic.

(B–C) Predicted tertiary structure of SYTA SMP domain modeled by alignment to the human E-SYT2 SMP domain (c4p42B) showing (B) frontal and (C) tunnel views. This secondary structure-based modeling predicts that the putative SYTA SMP domain would form the characteristic β-barrel comprising a highly twisted β-sheet and two α-helices, with a third helix partially capping one end of the barrel.

(D) Alignment of predicted SMP domains in Arabidopsis SYTA (aa 62-248), SYTB(aa 63-249), SYTC (aa 62-248), SYTD (aa 68-256) and SYTE (aa 71-257) with those in human (*H.s.*) E-SYT1 (aa 137-319), E-SYT2 (aa 187-370) and E-SYT3 (aa 115-296), and *S. cerevisiae* tricalbins Tcb1 (aa 209-375), Tcb2 (aa 165-372) and Tcb3 (aa 218-429). Generated using ClustW, with α-helix (orange) and β -strand (green) regions as predicted by Ali2D (http://toolkit.tuebingen.mpg.de). Note the polar and hydrophobic character of the predicted SMP domains in the Arabidopsis SYTs, and the characteristic conserved residues of an asparagine in the first α-helix, and bend-inducing glycines and prolines.

(E) Confocal images of SYTA-GFP and *S. cerevisiae* TagRFP-Ist2$^{490\text{-}946}$ expressed in *N. benthamiana* leaf epidermal cells showing SYTA and Ist2$^{490\text{-}946}$ co-localizing at ER nodes in the cell cortex. Scale bar as indicated.

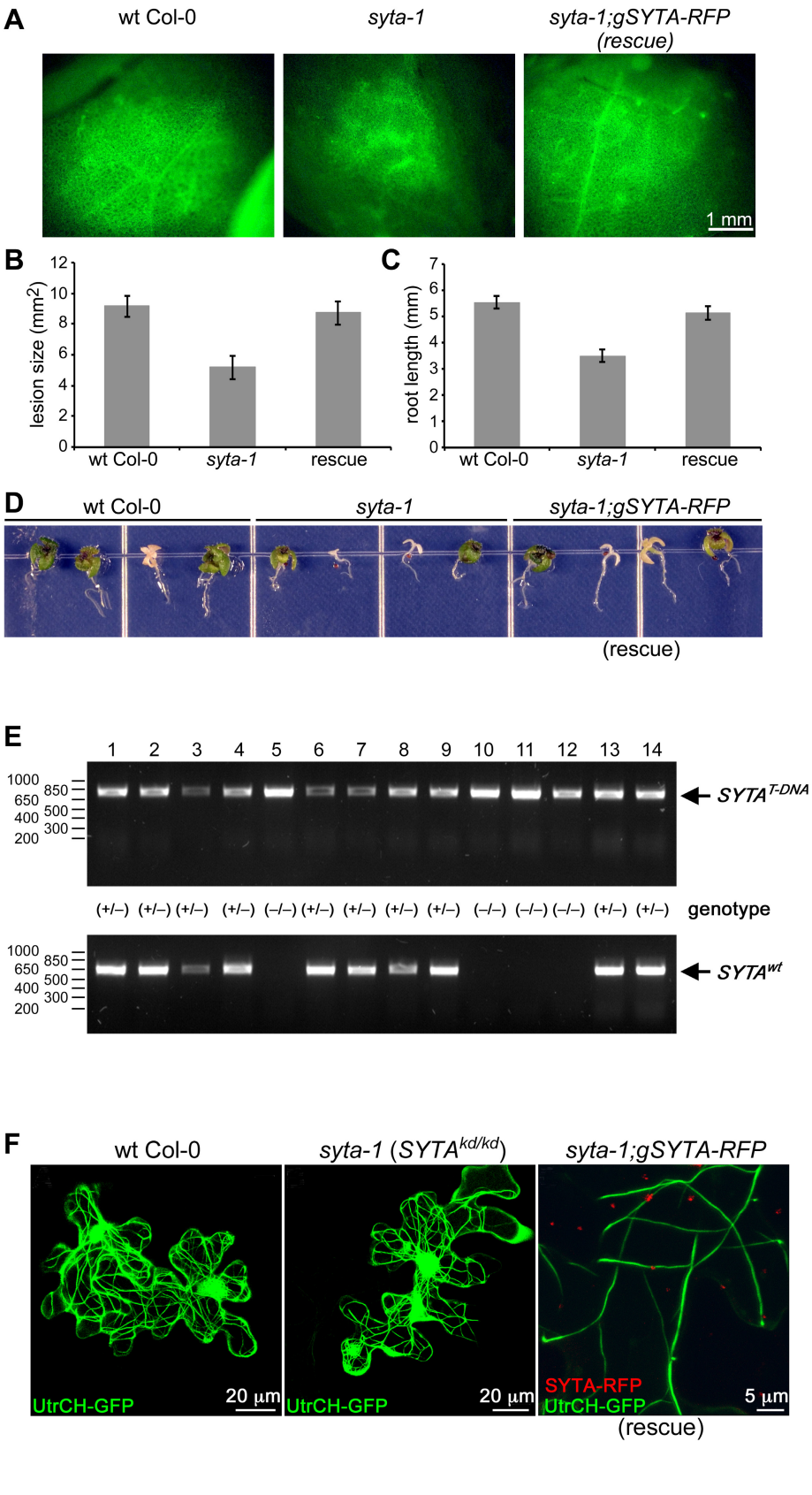
A
wt Col-0
syta-1
syta-1;gSYTA-RFP
(rescue)
1 mm
B
lesion size (mm2)
wt Col-0
syta-1
rescue
C
root length (mm)
wt Col-0
syta-1
rescue
D
wt Col-0
syta-1
syta-1;gSYTA-RFP
(rescue)
E
1 2 3 4 5 6 7 8 9 10 11 12 13 14
1000
650
400
200
850
500
300
SYTAT-DNA
(+/–) (+/–) (+/–) (+/–) (–/–) (+/–) (+/–) (+/–) (+/–) (–/–) (–/–) (–/–) (+/–) (+/–)
genotype
SYTAwt
F
wt Col-0
syta-1 (SYTAkd/kd)
syta-1;gSYTA-RFP
UtrCH-GFP
20 µm
UtrCH-GFP
20 µm
SYTA-RFP
UtrCH-GFP
5 µm
(rescue)

Figure S2. Full-length SYTA-RFP rescues the defective phenotypes of *syta*-1 and the actin cytoskeleton is not altered in *syta-1*. Related to Figure 1.

(A) Representative infection sites produced by infectious TVCV-GFP at 6 da pi on leaves of wt Col-0, *syta-1* and *SYTA-RFP* (*syta-1;gSYTA-RFP)* rescued line. Scale bar as indicated.

(B) Areas of infection sites at 6 da pi on leaves of wt Col-0, *syta-1* and *SYTA-RFP* rescued line inoculated with infectious TVCV-GFP. The areas of 37, 28 and 29 infection sites in wt, *syta-1* and SYTA-RFP, respectively, were measured (ANOVA and Tukey's HSD $P<0.001$).

(C) Root lengths of wt Col-0, *syta-1* and *SYTA-RFP* rescued line grown on 100 mM NaCl. Roots were measured at 20 da post-germination for 25 seedlings of each genotype (ANOVA and Tukey's HSD $P<0.001$).

(D) Representative seedlings of wt Col-0, *syta-1* and *SYTA-RFP* rescued line germinated on 100 mM NaCl.

(E) PCR genotyping of 14 F2 $kan^r/hyg^r/Basta^r$ segregant lines using primers specific for the *SYTA* coding region with (top panel) a T-DNA left border 3' primer to show the presence of the SAIL 775 A08 (*syta-1*) T-DNA insertion, and (bottom panel) a primer specific for the 3'UTR of the wt Col-0 *SYTA* locus to screen for the presence of wt *SYTA*. All lines were selected for presence of at least one T-DNA-mutated *syta-1* allele ($Basta^r$), and for the presence of *YFP-HDEL* (kan^r) and *gSYTA-RFP* (hyg^r). The absence of a wt *SYTA*-specific band (lower panel) identifies lines 5, 10, 11 and 12 as homozygous *syta-1* T-DNA insertion mutants (genotype –/–).

(F) Confocal images of the actin marker UtrCH-GFP transiently expressed in leaves of wt Col-0, *syta-1* and *SYTA-RFP* rescued line (*syta-1;gSYTA*-RFP) showing normal appearance of actin microfilaments in single leaf epidermal cells. Higher resolution confocal image of UtrCH-GFP expressed in *SYTA-RFP* rescued line (right panel) shows that endogenous SYTA does not co-localize with actin microfilaments. A few SYTA-RFP labeled ER-PM junctions may be associated with actin. Scale bar as indicated.

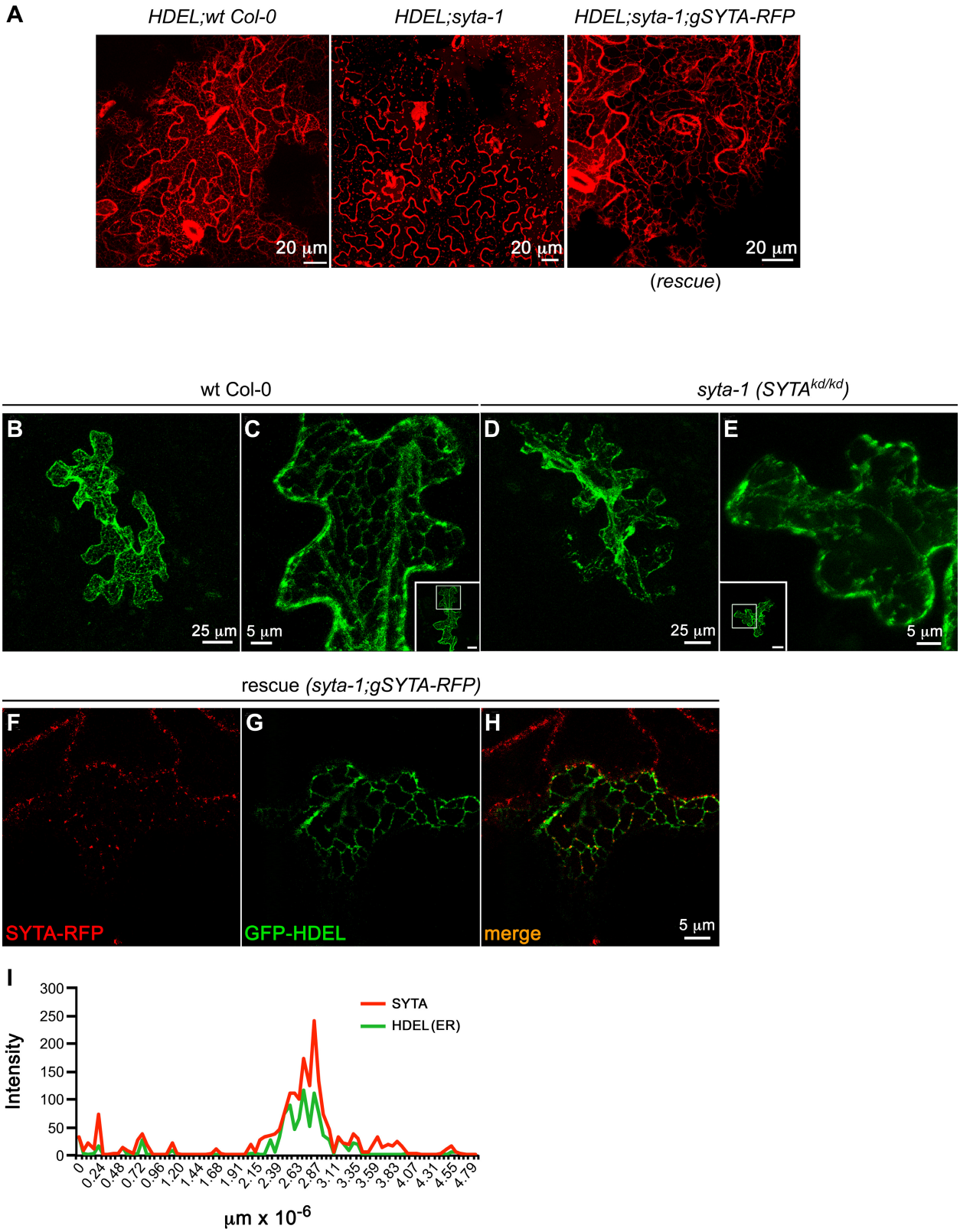
A
HDEL;wt Col-0
HDEL;syta-1
HDEL;syta-1;gSYTA-RFP
20 µm
20 µm
20 µm
(rescue)
wt Col-0
syta-1 (SYTA^kd/kd)
B
C
D
E
25 µm
5 µm
25 µm
5 µm
rescue (syta-1;gSYTA-RFP)
F
G
H
SYTA-RFP
GFP-HDEL
merge
5 µm
I
Intensity
300
250
200
150
100
50
0
SYTA
HDEL (ER)
0
0.24
0.48
0.72
0.96
1.20
1.44
1.68
1.91
2.15
2.39
2.63
2.87
3.11
3.35
3.59
3.83
4.07
4.31
4.55
4.79
µm x 10-6

Figure S3. SYTA is required for ER-PM tethering in Arabidopsis. Related to Figure 1.

(A) Confocal images of ER markers mCherry-HDEL endogenously expressed in stable transformants of Arabidopsis Col-0 wt, *syta-1* mutant or *SYTA-RFP* rescued (*syta-1;gSYTA-RFP*) lines showing (left) normal ER morphology in wt Col-0, (middle) fragmented appearance of the ER in *syta-1*, and (right) restoration of normal ER network morphology in *SYTA-RFP* rescued line (*syta-1;gSYTA-RFP*).

(B–H) Confocal images of the ER marker GFP-HDEL transiently expressed in Arabidopsis leaf epidermal cells. (B–E) are projected Z series.

(B–C) GFP-HDEL in Arabidopsis wt Col-0 leaf epidermal cells shows normal ER morphology and cortical ER network.

(D–E) GFP-HDEL in *syta-1* leaf epidermal cells shows the unstructured appearance of the ER collapsed in the interior of the cell.

(F–H) GFP-HDEL in leaf epidermal cells of the Arabidopsis rescue line *syta-1;gSYTA-RFP,* which expresses SYTA-TagRFP-T (SYTA-RFP), shows restoration of normal ER reticulate morphology and SYTA localized to cortical ER nodes at the plasma membrane (ER-PM junctions).

(I) Graph of fluorescence intensity of SYTA-TagRFP-T and GFP-HDEL at ER nodes from (G).

Scale bars as indicated.

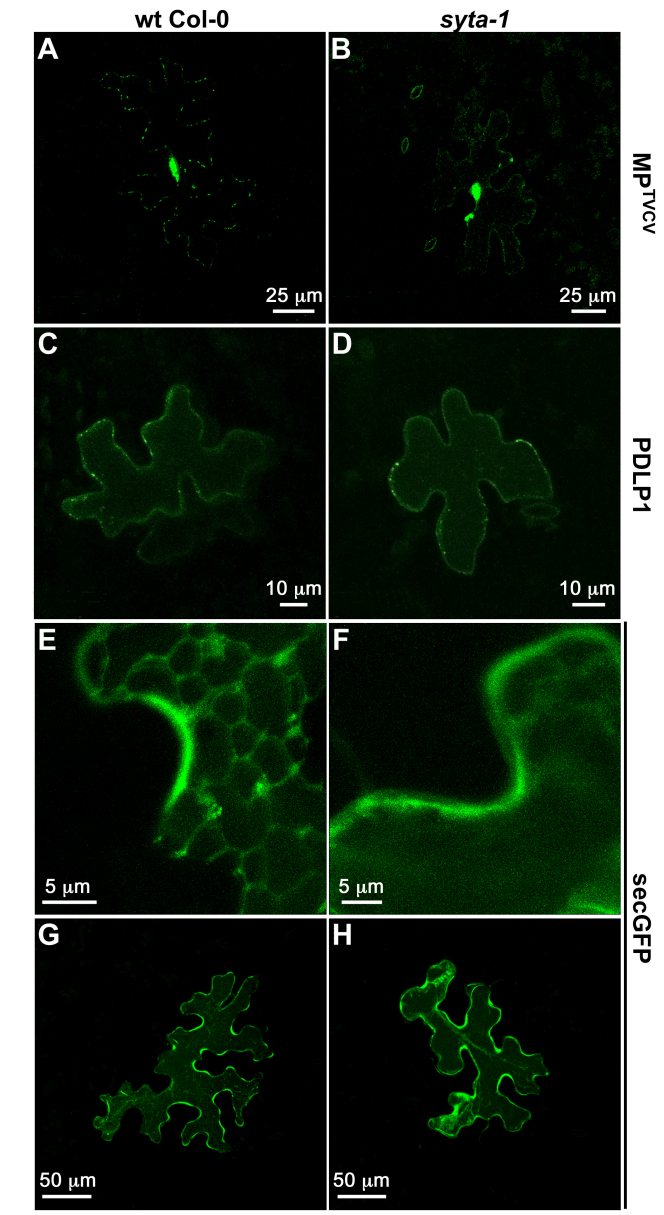
wt Col-0
syta-1
A
B
C
D
E
F
G
H
25 µm
25 µm
10 µm
10 µm
5 µm
5 µm
50 µm
50 µm
MP^TVCV
PDLP1
secGFP

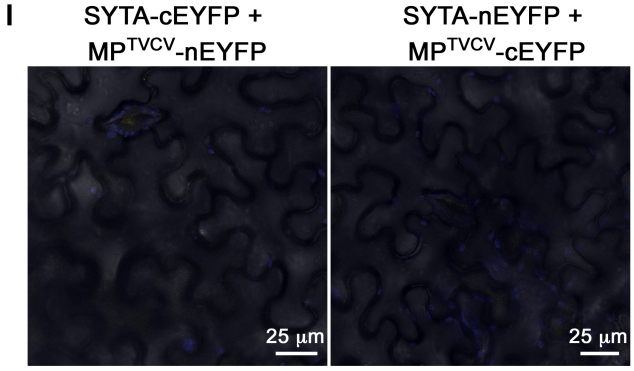
I
SYTA-cEYFP +
MP^TVCV-nEYFP
SYTA-nEYFP +
MP^TVCV-cEYFP
25 µm
25 µm

Figure S4. MP^{TVCV} trafficking to PD, but not PDLP1 trafficking to PD or secretory traffic, is inhibited in *syta-1*. Related to Figures 2, 3.

(A–B) Confocal images of MP^{TVCV}-GFP expressed in leaf epidermal cells of Arabidopsis wt Col-0 and *syta-1* plants showing MP^{TVCV} accumulates to lower levels at PD (punctae at plasma membrane) in *syta-1*.

(C–D) Confocal images of PDLP1-GFP in leaf epidermal cells of Arabidopsis wt Col-0 and *syta-1* plants showing PDLP1 accumulates at PD (punctae at plasma membrane) to comparable levels in both lines.

(E–H) Confocal images of a secreted form of GFP (secGFP) expressed in leaf epidermal cells of Arabidopsis wt Col-0 and *syta*-1 plants.

(E–F) show comparable incomplete secretion of GFP to the apoplasm in both lines at ~24 h post bombardment. Note secGFP levels in the apoplasm, and internally in the cortical ER network of wt cells or with an amorphous appearance in *syta-1* cells.

(G–H) show comparable accumulation of secreted GFP in the apoplasm in both lines at ~72 h post bombardment.

(I) BiFC of SYTA-nEYFP and MP^{TVCV}-cEYFP, and SYTA-cEYFP and MP^{TVCV}-nEYFP, co-expressed in *N. benthamiana* leaf epidermal cells. Neither pair produced YFP fluorescence, showing SYTA and MP^{TVCV} do not stably interact when transiently expressed in uninfected cells.

Scale bars as indicated.

Table S1: Primers used in this study. Related to Supplemental Experimental Procedures.

Construct	Primer Pairs or Primers[1]	Sequence (5' ➔ 3')
pCAMBIA1301::P_{SYTA}	5': 7-49-1983bpEcoRI	GGCGAATTCCCATTGTCCTTGCGAAGTGAGC
	3': 7-49-1bpNcoI	CCGCCCATGGTTTGATTTCCGTTTCAGATCCAAC
pCAMIBA1301::P_{SYTA}-gSYTA	5': 7-49UTRNotI	CCCCTCCAGCGGCCGCGAAGCGCACACAAAGTTTGCTTGC
	3': 7-49NcoI	CCCACCATGGAAGAGGCAGTTCGCCACTCGAGC
pCAMBIA1301::P_{SYTA}-gSYTA-TagRFP-T	5': TagRFPTFwdSacI	CCGGGCGGAGCTCGAGTGGCGAACTGCCTCGATGGTGTCTAAGGGCGAAGAGCTGA
	3': TagRFPTRevAflII	GCCTTAAGAAACTTTATTGCCAAATGTTTGAACGTTACTTGTACAGCTCGTCCATGCCAT
pTVCV::MP-cEYFP	5': TVCVMP5'EcoRI	CTGATGAATTCGTCGATTCGGTTGCAGCA
	3': PpuMI-cEYFP-3'	TCTGATGGGACCCTTACTTGTACAGCTCGTCCATGCC
pSITE::TagRFP-lst2$^{490-946}$	5': attlst2C	GGG GAC AAG TTT GTA CAA AAA AGC AGG CTT TTT TCC AAT CTA CGA TAA GC
	3': attlst2C	GGG GAC CAC TTT GTA CAA GAA AGC TGG GTC TTA AAG CTT CTT TTT CAG C
	SYTA 3'UTR	ACATAGTTTTTAACAACATCAAACCA
	5'LBsail	TTCATAACCAATCTCGATACA
	5'7-49a1133bp	GCTCTCTGAAGATAAGATTCC
	5'7-49bp1324	GCCTGACGAACATAAAGC

[1]Primer pairs to generate constructs as indicated. Last four listed primers were used to screen F2 segregating population from wt Col-0 HDEL-GFP x *syta;gSYTA-RFP* F1 lines for *HDEL-GFP;syta-1;gSYTA-RFP* lines that did not contain the wt *SYTA* locus.

Supplemental Experimental Procedures

Plant infectivity and expression assays. *N. benthamiana* plants were grown and maintained in growth chambers at 22°C under long-day (16 h light/8 h dark) conditions. Arabidopsis ecotype Col-0 plants were grown in growth rooms at 22°C under short-day (10 h light/14 h dark) conditions. We used biolistic bombardment or agroinfiltration with *Agrobacterium tumefaciens* GV2260 for transient expression assays in Arabidopsis or *N. benthamiana* leaves, respectively, as described [S1, S2], and assayed expression at ~40 h, unless otherwise noted. To transiently express proteins or markers in TVCV-infected cells, we inoculated 5-wk-old *N. benthamiana* leaves with a TVCV replicon and agroinfiltrated inoculated leaves 3 days later to introduce the appropriate plasmid. Arabidopsis and *N. benthamiana* leaves were inoculated with TVCV as described [S1] and cells were imaged 5 da after inoculation.

Cloning of expression plasmids and TVCV replicons. To construct the plasmid pCambia1301::P_{SYTA}-gSYTA-TagRFP-T containing the full-length SYTA genomic locus with its promoter, fused at its 3'-end to the sequence encoding Tag-RFP-T, we first PCR amplified the 1983 bp *SYTA* promoter region from Arabidopsis ecotype Col-0 DNA using primers *5'7-49-1983bpEcoRI* and *3'7-49-1bpNcoI*, and cloned this between the *Eco*RI and *Nco*I sites in pCAMBIA1301 to generate pCAMBIA1301::P_{SYTA} [S3]. We also PCR amplified the genomic *SYTA* coding sequence without its stop codon from Col-0 genomic DNA using primers *5'7-49UTRNotI* and *3'7-49NcoI*, and then cloned this into *Nco*I site in pCAMBIA1301::P_{SYTA} to generate pCAMBIA1301::P_{SYTA}-gSYTA [S3]. The *TagRFP-T* coding sequence was PCR amplified from pCP/TagRFP-T [S4] using forward primer *TagRFPTFwdSacI*, which contained the *SYTA* coding sequence starting at the SacI site (nt 3246), and reverse primer *TagRFPTRevAflII*, and then cloned between the *Sac*I and *Afl*II sites in pCAMBIA1301::P_{SYTA}-gSYTA to create pCAMBIA1301::P_{SYTA}-gSytA-TagRFP-T.

TVCV replicons expressing MP^{TVCV}-RFP and transient expression vectors expressing GFP- and RFP-tagged MP^{TVCV} have been described [S1]. We used Gateway vectors to generate transient expression vectors pSITE::SYTA-GFP and pSITE::SYTA-CFP. The *SYTA* cDNA coding sequence was PCR amplified from pBS-7-49CDS [S5], cloned into pDONR207 and then recombined into pSITE2NB or pSITE1NB destination vectors [S6]. To generate pSITE::SYTA-nEYFP, the *SYTA* cDNA coding sequence in pDONR207 was recombined into the destination vector pSITE-BiFC-nEYFP-N1 [S7]. To generate the TVCV replicon clone pTVCV::MP-cEYFP, the MP^{TVCV} coding sequence in pDONR207 [S1] was transferred into pSITE-BiFC-cEYFP-N1 to create pSITE::MP^{TVCV}-cEYFP. We then used primers *TVCVMP5'EcoRI* and *PpuMI-cEYFP-3'* to PCR amplify the 3'-fragment of the MP^{TVCV}-cEYFP fused sequence starting at nt 580 (internal *Eco*RI site) to add a 3′-terminal PpuMI site after the *cEYFP* stop codon, and cloned this between the EcoRI and PpuMI sites in pTVCV50, which contains the full-length infectious TVCV cDNA cloned under the control of the SP6 promoter [S8]. For TagRFP-Ist2$^{490-946}$ transient expression, nucleotides 1471-2841 of the *Saccharomyces cerevisiae Ist2* coding sequence were PCR amplified from pAM24 [S9] using primers *5'attIst2C* and *3'attIst2C*, and Gateway cloned into pDONR207, and then into the destination vector pSITEII 6C1 [S7] to create pSITE::TagRFP-Ist2$^{490-946}$.

All PCR primer pairs used in this study are listed in Table S1. All clones were verified by sequencing on an Applied Biosystems Automated 3730xl DNA Analyzer at the Sequencing Facility in the Cornell University Institute of Biotechnology.

Generation of transgenic lines. To generate *syta-1*;*gSYTA-RFP* rescue lines, we transformed our homozygous *syta-1* T-DNA line [S5] with pCAMBIA1301::P_{SYTA}- gSYTA-TagRFP-T using floral dip [S10] and used CLSM to screen for stable T1 progeny that expressed SYTA-RFP. Five lines identified from three independent transformations were characterized in detail and used for

quantitative studies: all exhibited the same pattern of SYTA-RFP localization and restoration of normal ER reticulate morphology, as assessed by transient expression of GFP-HDEL. All of our *SYTA-RFP* rescued lines (14 total studied) varied only in their relative levels of SYTA-RFP expression (low, medium or high). One medium and one high expressing line were also selfed to generate homozygous *gSYTA-RFP* lines. The pattern of SYTA-RFP expression was the same in our T1, T2 and T3 lines. To stably express the ER marker HDEL-YFP in these rescued lines, we crossed *syta-1*;*gSYTA-RFP* T2 progeny (homozygous for the *gSYTA-RFP* transgene) with the Arabidopsis Col-0 transgenic line ER-yk [S11]. Outcrossed progeny that expressed both SYTA-RFP and YFP-HDEL were selected by growth on kanamycin, hygromycin and Basta, and resistant seedlings were screened for the expression of both fusion proteins. F2 SYTA-RFP rescued progeny that expressed both YFP-HDEL and SYTA-RFP and were homozygous for the *syta-1* T-DNA insertion were identified by PCR screening of the F2 segregating population as previously described [S5], except that we used a 3' primer specific for the 3'UTR of the wt Col-0 *SYTA* locus (SYTA 3'UTR), rather than one for the 3' coding region, to screen for the presence of wt *SYTA*. Four lines among fourteen segregants were identified by screening and characterized (see Figure S2). Primers used for screening are listed in Table S1. We also stably expressed mCherry-HDEL in *syta-1*;*gSYTA-RFP* rescued lines, and in *syta-1* mutant lines and wt Col-0, by transforming these lines with the plasmid ER-rk using floral dip [S10, S11], and used CLSM to screen for T1 Basta^r/kan^r/hyg^r lines expressing the mCherry-HDEL marker. For the mCherry-HDEL transformant studies reported here, we used six *syta-1* lines from three independent transformations, four *SYTA-RFP* rescued lines from three independent transformations, and two wt Col-0 lines from two independent transformations. All gave the same results. To quantify co-occurrence and PCC, we counted from 12 to 22 cells per experiment for co-localization studies in *N. benthamiana*, and 26 to 33 cells per experiment for co-localization studies in Arabidopsis lines.

TVCV infectivity and salt stress assays. Local infection site assays for TVCV infectivity were done using *in vitro* genomic +RNA transcripts of TVCV-GFP, a full-length infectious clone of TVCV engineered to express free GFP from a duplicated copy of the viral coat protein gene promoter [S12]. Leaves of 5-wk-old wt Col-0, *syta-1* and *SYTA-RFP* rescued (*syta-1;gSYTA-RFP*) plants were mechanically inoculated with a standardized amount of TVCV +RNA and the sizes of infection sites were scored at 6 days pi. using a stereomicroscope and ImageJ software (http://rsbweb.nih.gov/ij/) as previously described [S1]. To assay root growth in response to high salt, wt Col-0, *syta-1* and *syta-1*;*gSYTA-RFP* seedlings were germinated on 0.1xMS medium containing 100mM NaCl under at 22°C under long-day (16 h light/8 h dark) conditions, and root length was measured at 20 da. We used a *SYTA-RFP* rescued line that was homozygous for the *gSYTA-RFP* transgene (SYTA-RFP expressed at medium levels) for these studies.

Protein accumulation in PD. To measure the levels of MP^{TVCV} and PDLP1 in PD, pSITE2NB::MP^{TVCV}-GFP or pB7FW2.0::PDLP1-GFP were biolistically bombarded into Arabidopsis Col-0 or *syta-1* leaf epidermal cells [S1, S2, S13] and cells were imaged at 18-24 h post bombardment. Images were imported into Photoshop, and the green fluorescence signal of MP^{TVCV}-labeled nuclei [S1] and chloroplast autofluorescence were eliminated. Protein integrated density in PD (punctae at the plasma membrane) was quantified using ImageJ software with the 'analyze particles' command (http://imagej.nih.gov/ij/). Detected particle size was set to 3-50 pixel^2 and the threshold adjusted to 50. Results were statistically analyzed by t-test using JMPPro 0.0.2 software (SAS, Cary, NC).

Microscopy. CLSM was performed using a Leica TCS SP5 spectral imaging system (Leica Microsystems, Wetzlar, Germany). GFP fluorescence was excited with a 488-nm argon laser, and emission was detected at 500 to 530 nm. RFP and mCherry fluorescence was excited with

a 561-nm diode-pumped solid-state (DPSS) laser, and emission was detected at 575 to 620 nm. YFP fluorescence was excited with a 514-nm argon laser, and emission was detected at 525-560 nm. CFP fluorescence was excited with a 458-nm argon laser, and emission was detected at 470 to 500 nm. Z series were collected at ~1-µm intervals and imaged using Leica software (Leica Microsystems). Fluorescence intensity graphs were generated using the LAS AF 2.4.1 software 'quantify intensity' tool (Leica Microsystems, Wetzlar, Germany). For co-localization studies, each fluorophore was scanned sequentially. Pearson's correlation coefficient (PCC) was calculated using Image-Pro Plus 6.3 software (Media Cybernetics, Rockville, MD) at the selected region of interest (ER nodes or PD). TVCV-GFP infection sites on inoculated leaves were identified by their fluorescence using an Olympus SZX-12 stereomicroscope (Olympus Corporation, Center Valley, PA) with a 480-/30-nm excitation filter and an 535-/40-nm emission filter.

Protein structure modeling. To predict the tertiary structure of the putative SYTA SMP domain, its predicted primary sequence was submitted to PHYRE2 (http://www.sbg.bio.ic.ac.uk/phyre2) to query the protein structure databases and the SYTA SMP domain structure was modeled based on the 3D structure of the *Hs*E-SYT2 SMP domain (c4p42B) at 100.% confidence. Structure prediction was further verified with MUSTER (http://zhanglab.ccmb.med.umich.edu/MUSTER) and RAPTOR (http://raptorx.uchicago.edu), and both gave identical results.

Supplemental References

S1. Levy, A., Zheng, J.Y., and Lazarowitz, S.G. (2013). The Tobamovirus *Turnip vein clearing virus* 30-kilodalton movement protein localizes to novel nuclear filaments to enhance virus infection. J. Virol. *87*, 6428-6440.

S2. Ueki, S., Lacroix, B., Krichevsky, A., Lazarowitz, S.G., and Citovsky, V. (2009). Functional transient genetic transformation of Arabidopsis leaves by biolistic bombardment. Nat. Protoc. *4*, 71-77.

S3. Lewis, J.D. (2006). Arabidopsis synaptotagmin SYTA regulates plant virus cell-to-cell transport and the formation of plasma membrane-derived endosomes. Ph.D. Thesis (Ithaca, NY: Cornell University), pp. 256.

S4. Shaner, N.C., Lin, M.Z., McKeown, M.R., Steinbach, P.A., Hazelwood, K.L., Davidson, M.W., and Tsien, R.Y. (2008). Improving the photostability of bright monomeric orange and red fluorescent proteins. Nature Meth. *5*, 545-551.

S5. Lewis, J.D., and Lazarowitz, S.G. (2010). Arabidopsis synaptotagmin SYTA regulates endocytosis and virus movement protein cell-to-cell transport. Proc. Natl. Acad. Sci. U.S.A. *107*, 2491-2496.

S6. Chakrabarty, R., Banerjee, R., Chung, S.M., Farman, M., Citovsky, V., Hogenhout, S.A., Tzfira, T., and Goodin, M. (2007). PSITE vectors for stable integration or transient expression of autofluorescent protein fusions in plants: probing *Nicotiana benthamiana*-virus interactions. MPMI *20*, 740-750.

S7. Martin, K., Kopperud, K., Chakrabarty, R., Banerjee, R., Brooks, R., and Goodin, M.M. (2009). Transient expression in *Nicotiana benthamiana* fluorescent marker lines provides enhanced definition of protein localization, movement and interactions in planta. Plant J. *59*, 150-162.

S8. Zhang, Y., Lartey, R.T., Hartson, S.D., Voss, T.C., and Melcher, U. (1999). Limitations to *Tobacco mosaic virus* infection of turnip. Arch. Virol. *144*, 957-971.

S9. Manford, A.G., Stefan, C.J., Yuan, H.L., Macgurn, J.A., and Emr, S.D. (2012). ER-to-plasma membrane tethering proteins regulate cell signaling and ER morphology. Dev. Cell *23*, 1129-1140.

S10. Clough, S.J., and Bent, A.F. (1998). Floral dip: a simplified method for Agrobacterium-mediated transformation of *Arabidopsis thaliana*. Plant J. *16*, 735-743.

S11. Nelson, B.K., Cai, X., and Nebenfuhr, A. (2007). A multicolored set of in vivo organelle markers for co-localization studies in Arabidopsis and other plants. Plant J. *51*, 1126-1136.

S12. Harries, P.A., Park, J.W., Sasaki, N., Ballard, K.D., Maule, A.J., and Nelson, R.S. (2009). Differing requirements for actin and myosin by plant viruses for sustained intercellular movement. Proc. Natl. Acad. Sci. U.S.A. *106*, 17594-17599.

S13. Thomas, C.L., Bayer, E.M., Ritzenthaler, C., Fernandez-Calvino, L., and Maule, A.J. (2008). Specific targeting of a plasmodesmal protein affecting cell-to-cell communication. PLoS Biology *6*, e7.